Inhibition and Promotion of Copper Corrosion by CTAB in a Microreactor System

Caroline M. Murira,[†] Christian Punckt,[†] Hannes C. Schniepp,[†] Boris Khusid,[‡] and Ilhan A. Aksay*,[†]

Department of Chemical Engineering, Princeton University, Princeton, New Jersey 08544, and Department of Chemical, Biological, and Pharmaceutical Engineering, New Jersey Institute of Technology, University Heights, Newark, New Jersey 07102

Received July 31, 2008. Revised Manuscript Received September 29, 2008

We report on an optical microscopy technique for the analysis of corrosion kinetics of metal thin films in microreactor systems and use it to study the role of cetyltrimethylammonium bromide surfactant as a corrosion inhibitor in a copper−gold galvanic coplanar microsystem. A minimum in the dissolution rate of copper is observed when the surfactant concentration is ∼0.8 mM. To explain why the inhibitory role of the surfactant does not extend to higher concentrations, we use zero resistance ammetry with separated half cells and show that while the surfactant inhibits cathodic reactions on gold, it also promotes the corrosion of copper because of the catalytic action of bromide counterions. These two competing processes lead to the observed minimum in the dissolution rate.

Introduction

Corrosion dynamics and inhibition of macroscopic bulk systems have been the focus of research for centuries and in many cases have been well analyzed and understood. A large number of powerful techniques are available to measure corrosion dynamics. Among these, electrochemical cell-based techniques stand out as the most widely used ones.[1−4] Electrochemical cell measurements not only provide corrosion current, corrosion potential, and corrosion resistance data for a system under investigation but also give insight into more fundamental properties such as reaction mechanisms, thermodynamics, and properties of surface films. On the negative side, a shortcoming of electrochemical cell experiments is that they lack spatial resolution.

Because of the increasing importance of microsystems (e.g., microelectromechanical systems)[5−7] and in the context of corrosion of dissimilar grains of composite materials,[8−11] there is a need for spatiotemporally resolved corrosion techniques for the study of localized corrosion. With the development of scanning electrochemical microscopy (SECM) and similar techniques, pioneered by Bard and co-workers,[12,13] spatially resolved images of the electrochemical properties of electrode surfaces could be obtained. While providing outstanding spatial resolution, SECM is based on the application of a voltage bias to the scanning microelectrode and therefore is not well suited for the analysis of freely corroding specimens. Scanning vibrating probe methods, the closely related scanning Kelvin probe technique, and the scanning reference electrode techniques are better suited for this purpose.[8,14−17] However, while providing quantitative spatiotemporally resolved data, their spatial resolution is rather low. More importantly, the presence of a (vibrating) scanning electrode in close distance to the analyzed surface often constitutes a strong perturbation to the system which complicates data analysis.[18−20]

Here, we present a novel, noninvasive method based on simple optical microscopy for spatiotemporally resolved corrosion rate measurements in specially designed model systems. The spatial resolution is determined by the optical properties of the setup (i.e., the numerical aperture of the lens used for imaging). The sensitivity of the method in terms of local current density is mainly determined by fluctuations of the illumination, noise generated by the image recording setup, and the time interval between subsequent recorded images. In our case, the sensitivity lies on the order of 50 μA/cm^2 but can easily be improved (e.g., by employing a cooled CCD camera).

We demonstrate the usefulness and capabilities of our setup by measuring the dissolution dynamics of copper thin films on gold substrates. Since our long-range goal is to understand the role of surfactants in corrosion inhibition, we use this technique

* Corresponding author. Phone: (609) 258-4393. E-mail: iaksay@princeton.edu.

[†] Princeton University.

[‡] New Jersey Institute of Technology.

(1) Bard, A. J.; Stratmann, M.; Frankel, G. S. *Corrosion and Oxide Films*; Wiley-VCH: Weinheim, Germany, 2003; Vol. 4.

(2) Bockris, J. O. M.; Reddy, A. K. N. *Modern Electrochemistry*, 2nd ed.; Kluwer Academic Publishers: New York, 2004.

(3) Evans, U. R. *The Corrosion and Oxidation of Metals: Scientific Principles and Practical Applications*; Edward Arnold: London, 1960.

(4) Jones, D. A. *Principles and Prevention of Corrosion*, 2nd ed.; Prentice Hall: Upper Saddle River, NJ, 1996.

(5) Miller, D. C.; Hughes, W. L.; Wang, Z. L.; Gall, K.; Stoldt, C. R. *J. Microelectromech. Syst.* **2007**, *16*, 87–101.

(6) Pierron, O. N.; Macdonald, D. D.; Muhlstein, C. L. *Appl. Phys. Lett.* **2005**, *86*, 211919.

(7) Kahn, H.; Deeb, C.; Chasiotis, I.; Heuer, A. H. *J. Microelectromech. Syst.* **2005**, *14*, 914–923.

(8) Jorcin, J. B.; Blanc, C.; Pebere, N.; Tribollet, B.; Vivier, V. *J. Electrochem. Soc.* **2008**, *155*, C46–C51.

(9) Blanc, C.; Freulon, A.; Lafont, M. C.; Kihn, Y.; Mankowski, G. *Corros. Sci.* **2006**, *48*, 3838–3851.

(10) Jones, R. H.; Baer, D. R.; Danielson, M. J.; Vetrano, J. S. *Metall. Mater. Trans. A* **2001**, *32*, 1699–1711.

(11) Yasakau, K. A.; Zheludkevich, M. L.; Lamaka, S. V.; Ferreira, M. G. S. *Electrochim. Acta* **2007**, *52*, 7651–7659.

(12) Bard, A. J.; Fan, F. R. F.; Kwak, J.; Lev, O. *Anal. Chem.* **1989**, *61*, 132–138.

(13) Bard, A. J.; Fan, F. R. F.; Pierce, D. T.; Unwin, P. R.; Wipf, D. O.; Zhou, F. M. *Science* **1991**, *254*, 68–74.

(14) Femenia, M.; Canalias, C.; Pan, J.; Leygraf, C. *J. Electrochem. Soc.* **2003**, *150*, B274–B281.

(15) Guillaumin, V.; Schmutz, P.; Frankel, G. S. *J. Electrochem. Soc.* **2001**, *148*, B163–B173.

(16) Lacroix, L.; Ressier, L.; Blanc, C.; Mankowski, G. *J. Electrochem. Soc.* **2008**, *155*, C8–C15.

(17) Schmutz, P.; Frankel, G. S. *J. Electrochem. Soc.* **1998**, *145*, 2295–2306.

(18) Breuer, N.; Stimming, U.; Vogel, R. *Electrochim. Acta* **1995**, *40*, 1401–1409.

(19) Isaacs, H. S. *J. Electrochem. Soc.* **1991**, *138*, 722–728.

(20) McMurray, H. N.; Williams, D.; Worsley, D. A. *J. Electrochem. Soc.* **2003**, *150*, B567–B573.

10.1021/la8024759 CCC: $40.75

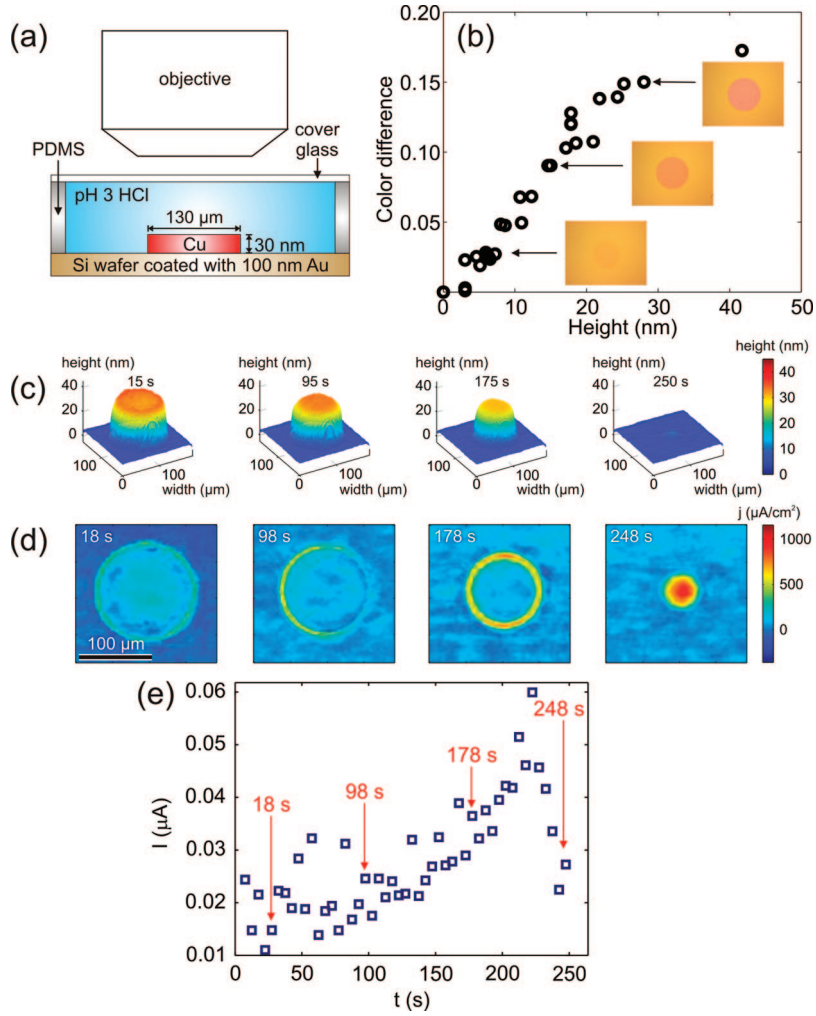

Figure 1. (a) Sketch of the experimental setup. (b) Height vs color difference calibration curve (see SI for further explanation). (c) Copper disk dissolving in pH 3 HCl showing change in height and width as a function of time. (d) Estimated current density j of dissolving copper disk as a function of time. (e) Total current I of dissolving copper disk as a function of time.

to study the effect of cetyltrimethylammonium bromide (CTAB) surfactant as a corrosion inhibitor. Dating back to the pioneering work of Manne and Gaub,[21,22] adsorption characteristics of surfactants (including CTAB) on model surfaces such as gold, mica, and highly oriented graphite have been studied by scanning probe microscopic techniques and are now well understood.[23−33] Surfactants, and in particular CTAB, have been used to hinder the corrosion of various metals, and many of the mechanisms by which corrosion inhibition takes place are understood.[34−43] In our study, however, we investigate the corrosion behavior of copper in combination with a dissimilar gold cathode in a microsystem, which, to our knowledge, has not been reported in the literature. Also, the application of spatiotemporally resolving techniques to study the role of surfactants in corrosion prevention has not been demonstrated. Our optical microscopy studies show that as the CTAB concentration increases to 0.8 mM, corrosion inhibition increases, while above this concentration, inhibition becomes weaker. This means that, at high CTAB concentrations, additional effects must come into play that have a promoting effect on the corrosion reactions.

To understand this dual role of CTAB as a corrosion inhibitor and promoter, we complement our optical measurements with zero resistance ammetry (ZRA) and atomic force microscopy

(21) Manne, S.; Cleveland, J. P.; Gaub, H. E.; Stucky, G. D.; Hansma, P. K. *Langmuir* **1994**, *10*, 4409–4413.
(22) Manne, S.; Gaub, H. E. *Science* **1995**, *270*, 1480–1482.
(23) Ducker, W. A.; Wanless, E. J. *Langmuir* **1999**, *15*, 160–168.
(24) Grant, L. M.; Tiberg, F.; Ducker, W. A. *J. Phys. Chem. B* **1998**, *102*, 4288–4294.
(25) Wanless, E. J.; Ducker, W. A. *J. Phys. Chem.* **1996**, *100*, 3207–3214.
(26) Jaschke, M.; Butt, H. J.; Gaub, H. E.; Manne, S. *Langmuir* **1997**, *13*, 1381–1384.
(27) Manne, S.; Schaffer, T. E.; Huo, Q.; Hansma, P. K.; Morse, D. E.; Stucky, G. D.; Aksay, I. A. *Langmuir* **1997**, *13*, 6382–6387.
(28) Burgess, I.; Jeffrey, C. A.; Cai, X.; Szymanski, G.; Galus, Z.; Lipkowski, J. *Langmuir* **1999**, *15*, 2607–2616.
(29) Xu, S. M.; Chen, M. H.; Cholewa, E.; Szymanski, G.; Lipkowski, J. *Langmuir* **2007**, *23*, 6937–6946.
(30) Saville, D. A.; Chun, J.; Li, J. L.; Schniepp, H. C.; Car, R.; Aksay, I. A. *Phys. Rev. Lett.* **2006**, *96*, 018301.
(31) Schniepp, H. C.; Saville, D. A.; Aksay, I. A. *J. Am. Chem. Soc.* **2006**, *128*, 12378–12379.
(32) Schniepp, H. C.; Saville, D. A.; Aksay, I. A. *Langmuir* **2008**, *24*, 626–631.
(33) Schniepp, H. C.; Shum, H. C.; Saville, D. A.; Aksay, I. A. *J. Phys. Chem. B* **2007**, *111*, 8708–8712.
(34) Abd El-Maksoud, S. A. A. *J. Electroanal. Chem.* **2004**, *565*, 321–328.
(35) Amin, M. A. *J. Appl. Electrochem.* **2006**, *36*, 215–226.
(36) Atia, A. A.; Saleh, M. M. *J. Appl. Electrochem.* **2003**, *33*, 171–177.
(37) Elachouri, M.; Hajji, M. S.; Salem, M.; Kertit, S.; Aride, J.; Coudert, R.; Essassi, E. *Corrosion* **1996**, *52*, 103–108.
(38) Li, X. H.; Mu, G. N. *Appl. Surf. Sci.* **2005**, *252*, 1254–1265.
(39) Luo, H.; Guan, Y. C.; Han, K. N. *Corrosion* **1998**, *54*, 619–627.
(40) Ma, H. Y.; Chen, S. H.; Yin, B. S.; Zhao, S. Y.; Liu, X. Q. *Corros. Sci.* **2003**, *45*, 867–882.
(41) Maayta, A. K.; Bitar, M. B.; Al-Abdallah, M. M. *Br. Corros. J.* **2001**, *36*, 133–135.
(42) Mu, G. N.; Zhao, T. P.; Liu, M.; Gu, T. *Corrosion* **1996**, *52*, 853–856.
(43) Zhao, T. P.; Mu, G. N. *Corros. Sci.* **1999**, *41*, 1937–1944.

(AFM) and show that the role of CTAB as both a corrosion inhibitor and promoter relates to its different functions on the cathode and the anode. On gold, CTAB serves as a corrosion inhibitor by blocking the cathodic reactions. However, while it is blocking the cathodic reactions, it simultaneously promotes reactions on the copper anode. The competition between these two effects yields a minimum in the corrosion rate since the inhibitive effect of CTAB on gold saturates.

Experimental Section

Experiments were conducted using a well-defined model system that consists of disk-shaped copper thin films with 130-μm diameter that were electrolessly plated on a gold electrode (Figure 1a). The gold electrode was prepared by subsequent evaporation of 10 nm of titanium and 100 nm of gold on a silicon wafer using an e-beam evaporator (Denton DV-502A, Denton Vacuum). Before each experiment, this coplanar galvanic couple was pre-etched in pH 3 HCl solution for about 10 s to remove unwanted surface oxide layers.

In our optical copper dissolution experiments, these samples were immersed in a pH 3 HCl solution and observed with bright-field (BF) optical microscopy (Zeiss Axioplan 2, Carl Zeiss MicroImaging, Inc.). The cell volume was enclosed by a 5-mm-thick poly(dimethylsiloxane) spacer that was placed on the gold electrode and covered by a microscope cover glass.

To test the possibility of obtaining quantitative dissolution data from optical images, a series of calibration measurements were performed. For this purpose, copper thin films with varying thicknesses were prepared. Their height was measured with a surface profiler (KLA-Tencor). Then BF images of the thin films were taken, and their color was analyzed. Up to a thickness of 40 nm, we found an approximately linear relationship between the color of a copper island and its thickness as illustrated in Figure 1b. Details of the calibration can be found in the Supporting Information (SI). Thus, by observing corroding metal thin films with a thickness of less than or equal to 40 nm, we can in situ monitor the time evolution of the film thickness using optical microscopy.

Images were recorded using a 12-bit digital CCD camera (Zeiss AxioCam HRc, Carl Zeiss MicroImaging, Inc.) and stored in a computer for further analysis. Using MatLab image analysis tools, we calculated a spatially resolved map of the copper thickness from the specific color values in a time sequence of images. Approximate dissolution rates were estimated by calculating the temporal derivative of the thickness data.

To confirm our microscopy data with independent experimental methods, we performed in situ AFM experiments (Multimode Nanoscope IIIA, Veeco) and ZRA (SP-150, Bio-Logic USA). The electrodes for AFM measurements were fabricated as described above. For ZRA measurements, we used a high purity copper rod with a nominal diameter of 3.175 mm (1/8 in.) as a working electrode. The rod was embedded in epoxy, ground, polished with 1000 grit polishing paper, and cleaned by ultrasonication in acetone and subsequent rinsing in Picopure DI water. Before the experiment, it was wiped with concentrated nitric acid and rinsed again with DI water. As a counter electrode, an evaporated gold film (30 mm $\times$ 38 mm) was used which was cleaned by etching in Piranha solution before the experiment.

Reaction products forming on the copper films during the experiment were analyzed ex situ by Fourier transform infrared spectroscopy (FTIR) (Nexus 670, Thermo Fisher Scientific, Inc.). All solutions and chemicals used were prepared with reagent-grade chemicals and Picopure water with a measured resistivity > 18 MΩ/cm.

Results and Discussion

First, we present in situ topography measurements and spatially resolved dissolution rates for a copper disk dissolving in a pH 3 HCl solution. Next, we compare optical microscope images of a copper disk dissolving in the pH 3 HCl solution with a disk dissolving in a CTAB solution at varying surfactant concentrations and quantify the inhibitory effect of the surfactant. Lastly, we verify the spatiotemporal dissolution dynamics of a copper disk in HCl solution using AFM, and we confirm the presence of a minimum in dissolution rate as a function of CTAB concentration using ZRA measurements for bulk electrodes. On the basis of the ZRA measurements, we propose a mechanism for the minimum in dissolution rate as a function of CTAB concentration for the copper−gold galvanic microreactor.

Spatiotemporally Resolved Corrosion Studies by Optical Microscopy. As our galvanic cell comes into contact with the HCl electrolyte, Faradaic reactions on copper anode and gold cathode lead to the dissolution of the copper disk. While reactions on both electrodes can be rather complex, especially in the presence of catalytically active chloride ions which form complexes with dissolving copper ions, we can write down basic reaction equations that illustrate the electrode processes on anode and cathode. In the presence of oxygen in the electrolyte, a direct formation of cupric ions (Cu^{2+}) is unlikely to play a major role. According to Bech-Nielsen et al.[44] and references therein, for our system the dissolution of the copper metal is more likely to occur through the formation of cuprous chloride species and subsequent oxide formation:

$$\mathrm{Cu} + 2\mathrm{Cl}^- \rightleftarrows \mathrm{CuCl}_{2,\mathrm{ads}}{}^- + \mathrm{e}^-$$

$$2\mathrm{CuCl}_{2,\mathrm{ads}}{}^- + \mathrm{H_2O} \rightleftarrows \mathrm{Cu_2O_{ads}} + 2\mathrm{H}^+ + 4\mathrm{Cl}^- \qquad (1)$$

Depending on the conditions in solution, cuprous oxide can dissolve in the electrolyte. Furthermore, in addition to the electrochemical processes, nonelectrochemical dissolution of the copper electrode can occur at an initial stage of the dissolution process which leads to a local increase of the electrolyte acidity. Details of the reaction mechanisms can be found in the literature.[44,45] In the specific case of our galvanic system, the electrochemical dissolution of copper is balanced by an oxygen reduction reaction taking place mainly on the gold cathode:[46,47]

$$\mathrm{O_2} + 2\mathrm{H}^+ + 2\mathrm{e}^- \rightleftarrows \mathrm{H_2O_2} \qquad (2)$$

Topographical changes during the dissolution of a copper disk with a diameter of 130 μm and a height of about 30 nm are shown in Figure 1c. From the color of the dissolving copper electrode, we can calculate its approximate thickness by linear interpolation between the color of the gold cathode and the initial color of the copper. By calculating the difference between thickness data at subsequent time moments, a dissolution rate in nanometers per second as well as a current density can be estimated (Figure 1d), given that Cu^+ ions are the electrochemically active species on the anode. As expected for a rather low conductivity electrolyte (pH 3 HCl has a conductivity of about 200 μS/cm), the reaction is strongly localized at the rim of the copper disk (t = 18 s). After 178 s, the reaction zone has broadened, and at t = 248 s, the current density is almost uniform. Since we cannot apply any stirring in our microsystem, this change can probably be explained by a local increase of the electrolyte conductivity caused by the accumulation of reaction products and chloride ions close to the electrode surface. This claim is supported by experiments (not shown) in which the galvanic cell is swirled in a pH 3 HCl solution for defined time intervals and examined under the microscope ex situ after drying

(44) Bech-Nielsen, G.; Jaskula, M.; Chorkendorff, I.; Larsen, J. *Electrochim. Acta* **2002**, *47*, 4279–4290.
(45) Bjorndahl, W. D.; Nobe, K. *Corrosion* **1984**, *40*, 82–87.
(46) Genshaw, M. A.; Damjanov, A.; Bockris, J. O. *J. Electroanal. Chem.* **1967**, *15*, 163–172.
(47) Hamann, C. H.; Hamnett, A.; Vielstich, W. *Electrochemistry*; Wiley-VCH: Weinheim, Germany, 1998.

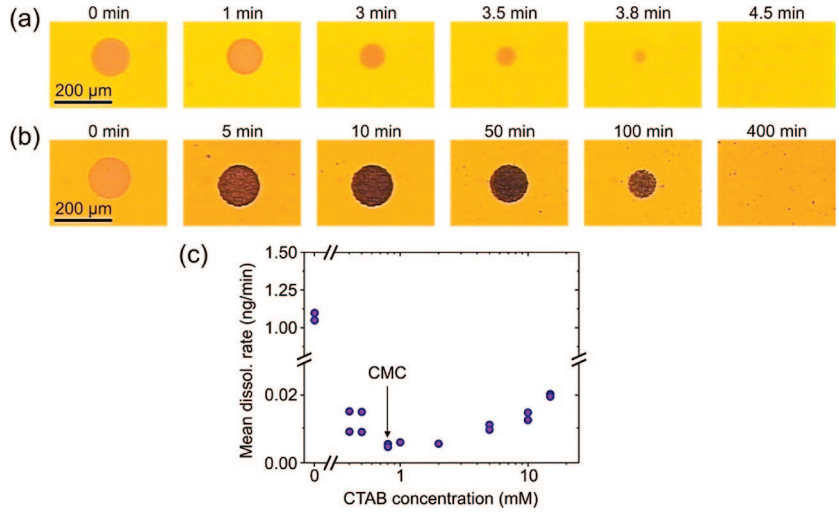

Figure 2. Performance of CTAB as a corrosion inhibitor in a copper−gold galvanic pair. (a) Optical microscope images of a copper disk dissolving in pH 3 HCl. (b) Optical microscope images of a copper disk dissolving in pH 3 HCl with 0.4 mM CTAB. (c) Average dissolution rate of copper disks in pH 3 HCl with different concentrations of CTAB.

under a flow of nitrogen. In this case, the dissolution proceeds more slowly and almost no broadening of the reaction zone occurs compared to the microsystem. Thus, electrochemically active species accumulating at the dissolving copper anode must have an autocatalytic effect leading to a higher corrosion rate in the galvanic microreactor. Because of the small scale of our galvanic system, the dissolving copper disk is comparable to a corrosion pit, where the accumulation of aggressive species is known to lead to an autocatalytically induced spreading of corrosion reactions.[48]

In addition to the radial heterogeneity of the current density, we observe an angular dependence as well. This is due to a small mechanical vibration of the microscope stage. As the stage is slightly shifting, it appears as if the current density is increased on one side of the disk and decreased on the other. Similar effects, however, could be caused by convection of the electrolyte as well.

As a result of the heterogeneous current density, the copper electrode dissolves from the rim inward. While the outer parts of the copper island have already corroded away, the thickness at the center of the island is only slightly changed (Figure 1c, $t = 95$ s). This heterogeneity is a result of our coplanar electrode geometry and is typical for the corrosion of dissimilar metals which are immersed in low conductivity electrolyte.[3,4]

We can obtain an estimate for the global anodic current by the spatial integration of the current density. The obtained current is plotted in Figure 1e as a function of time. While the broadening of the reaction zone is taking place, the total current slowly increases. After 220 s, the current reaches a maximum and then decays to zero as the copper island disappears completely ($t =$ 250 s). We attribute the increase in current to the aforementioned local conductivity increase. In a simple picture, a reduced ohmic potential drop between anodic and cathodic sites increases the overpotentials on anode and cathode and thus increases the reaction rates.[49]

In a second step, we applied our optical method to the analysis of corrosion inhibition by CTAB. The dissolution of copper thin film islands in the absence and presence of CTAB is shown in Figure 2a,b. In the presence of CTAB, a strong color change of the copper island is observed. Below, we characterize the height change by AFM and show that this discoloration is due to the formation of an adlayer forming on the copper disk. Although this makes a quantitative analysis of height change, dissolution rate, and current density impossible, we can still measure and compare the time it takes to completely dissolve the copper structures. These optically determined average dissolution times are sufficient to determine the average dissolution rate since the amount of copper in the system is known. Also, the discoloration provides additional information about the corrosion processes taking place on the copper electrode since it indicates that the formation of a reaction product layer in the presence of the inhibitor might play a role in the inhibition mechanism. The discoloration is only observed in the presence of the surfactant.

The average dissolution rate as a function of the concentration of CTAB is shown in Figure 2c. The dissolution rate decreases up to a CTAB concentration of 0.8 mM which is the bulk CMC of CTAB in pure water (Atkin and co-workers show that for CTAB the CMC is almost independent of pH[50]). This corresponds to an increase in corrosion inhibition efficiency (IE) up to the CMC and has been observed using classical techniques in a variety of systems.[34−43,51] Corrosion IE can be calculated using the following formula where R_0 denotes the dissolution rate in the absence of the inhibitor and R_{inh} the dissolution rate when the inhibitor is present:

$$\mathrm{IE}(\%) = \left(\frac{R_0 - R_{\mathrm{inh}}}{R_0}\right) \cdot 100 \qquad (3)$$

The maximum IE calculated at the CMC of CTAB from the dissolution rates shown in Figure 2c and using eq 3 is 99.5%. This maximum IE is significantly higher than the reported value

(48) Punckt, C.; Bolscher, M.; Rotermund, H. H.; Mikhailov, A. S.; Organ, L.; Budiansky, N.; Scully, J. R.; Hudson, J. L. *Science* **2004**, *305*, 1133–1136.

(49) The consistency of our analysis can be tested by integrating the global current and calculating the corresponding mass of dissolved copper ions (taking into account Cu^+ as the only charge-carrying species) using Faraday's law. Alternatively, the mass of the copper island can be calculated from its known geometry (disk with 70-μm diameter and 30-nm height). From the current curve, we obtain a copper mass of about 4.6 ng, which is in good agreement with the 4.2 ng calculated from the island shape. In addition to Faradaic contributions to the metal dissolution, however, also non-Faradaic processes could dissolve the material. This would be detected by our optical method as well. While in our system such processes are not expected to play a significant role, in other systems, the calculation of a local rate of mass loss might be more accurate than the calculation of a current density.

(50) Atkin, R.; Craig, V. S. J.; Biggs, S. *Langmuir* **2000**, *16*, 9374–9380.

(51) Ashassi-Sorkhabi, H.; Majidi, M. R.; Seyyedi, K. *Appl. Surf. Sci.* **2004**, *225*, 176–185.

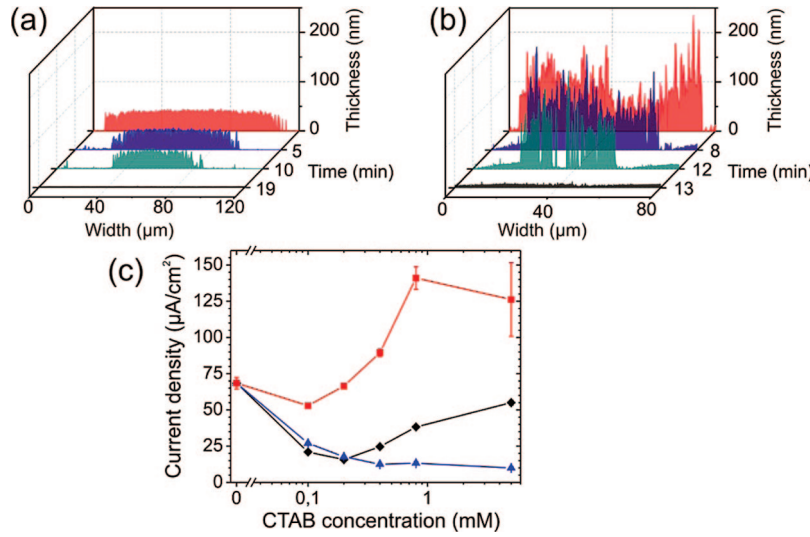

Figure 3. AFM profiles and ZRA data. (a) Thickness of a copper disk dissolving in pH 4.8 HCl as a function of time measured by AFM scans across the center of the disk. (b) Thickness of a copper disk dissolving in pH 3 HCl with 0.4 mM CTAB as a function of time (AFM scans). (c) Current density as a function of CTAB concentration obtained from ZRA experiments with separated half cells. Black diamonds represent CTAB in both half cells, blue triangles represent CTAB in the gold half cell only, and red squares represent CTAB in the copper half cell only. Error bars indicate scatter in measured current values.

of around 98% in the literature using electrochemical cell measurements for CTAB inhibiting the corrosion of copper at the corrosion potential in sulfuric acid.[52] The corrosion rate at maximum IE of 99.5% will be $0.005 \times R_0$, whereas the corrosion rate at maximum IE of 98% will be $0.02 \times R_0$. In other words, the expected lifetime of a copper specimen is four times longer at an IE of 99.5% compared to an IE of 98%.

This discrepancy between the literature data and our result can be due to three different factors. First, and most importantly, we analyze copper dissolution in HCl solution. There is little reason to expect similar inhibition efficiency of a certain inhibitor in different chemical environments since surface charge of the copper and adsorption properties of the surfactant are probably different. Second, our galvanic cell is a microreactor. Because of the coplanar electrode configuration, electrolyte resistance and diffusion limits for ion transport can be expected to have different values compared to chemically similar bulk systems. Third, the formation of reaction products on the copper surface during the dissolution process might cause a systematic error: Reaction products (such as copper chloride or cuprous oxide[53−57]) might be present on the surface long after the metallic copper has been dissolved. Thus, we would systematically measure larger dissolution times and thus larger IE. These differences are discussed further in the ZRA section.

The increase in the dissolution rate above the CMC has been reported for a few bulk metal and surfactant combinations[40−42] and is rather counterintuitive if it is assumed that the surfactant adsorbs uniformly on the surface of the metal. Adsorption data show that the surface concentration of the surfactant increases with increasing bulk concentration and reaches saturation at the CMC.[58,59] If the bulk concentration is further increased, the surface concentration remains constant. Consequently, the corrosion inhibition provided by the surfactant layer should reach a maximum at the CMC and remain constant after that. In fact, this saturation behavior is commonly observed for a variety of surfactant molecules acting as corrosion inhibitors.[35−37,39−41,43]

However, the observed increase in dissolution rate beyond the CMC indicates that, in addition to the expected inhibitory effect due to blocking and poisoning of the electrode surfaces (either anode or cathode), the CTAB must also have a detrimental effect at least at concentrations above the CMC if not at all concentrations. To explain this observation, Ma et al.[52] suggested that the specific adsorption of catalytically active bromide counterions from CTAB molecules on the copper electrode promotes corrosion at surfactant concentrations above 1 mM. This role of halide ions as corrosion promoters has previously been described in the literature.[53,57] In our ZRA experiments presented below, we show that CTAB has an additional promoting effect on copper corrosion in our system already at concentrations below 1 mM and that the observed inhibition above 0.1 mM mainly has a cathodic origin.

Spatiotemporally Resolved Corrosion Studies by Atomic Force Microscopy. To corroborate our results based on optical measurements, we performed in situ AFM imaging of our corroding copper thin films. AFM scans across a corroding copper island are shown in Figure 3a. In the absence of surfactant molecules, the observed dissolution dynamics are qualitatively the same as the ones observed with the optical technique (compare to Figure 1c): We again observe dissolution from the edge of the island toward its center, as expected for low conductivity electrolytes.

In the presence of CTAB, however, the thickness of the island is substantially larger (Figure 3b); since the thickness of the copper film is the same as in the experiments without the corrosion inhibitor, surfactant molecules apparently cause the formation of a thick layer on the copper anode already at concentrations below the CMC. Ex situ FTIR measurements indicate that this layer consists of a composite of organic (presumably surfactant) molecules and reaction products such as cuprous oxide (see SI).

(52) Ma, H. Y.; Chen, S. H.; Zhao, S. Y.; Liu, X. Q.; Li, D. G. *J. Electrochem. Soc.* **2001**, *148*, B482–B488.
(53) Aben, T.; Tromans, D. *J. Electrochem. Soc.* **1995**, *142*, 398–404.
(54) Barcia, O. E.; Mattos, O. R.; Pebere, N.; Tribollet, B. *J. Electrochem. Soc.* **1993**, *140*, 2825–2832.
(55) Braun, M.; Nobe, K. *J. Electrochem. Soc.* **1979**, *126*, 1666–1671.
(56) Feng, Y.; Siow, K. S.; Teo, W. K.; Tan, K. L.; Hsieh, A. K. *Corrosion* **1997**, *53*, 389–398.
(57) Tromans, D.; Sun, R. H. *J. Electrochem. Soc.* **1991**, *138*, 3235–3244.
(58) Atkin, R.; Craig, V. S. J.; Wanless, E. J.; Biggs, S. *Adv. Colloid Interface Sci.* **2003**, *103*, 219–304.
(59) Benton, D. P.; Sparks, B. D. *Trans. Faraday Soc.* **1967**, *63*, 2270–2274.

Details of the reactions leading to the formation of the thick layer are still under investigation and will not be discussed further here since the lack of this information does not affect the conclusions of the article.

The AFM scans in the absence of CTAB had to be conducted in a pH 4.8 HCl solution instead of a pH 3 HCl solution to slow the dissolution reaction. This was necessary, since AFM is an intrinsically slow method on a length scale of more than 100 μm, and dissolution at pH 3 would happen so rapidly that it could not be properly recorded. Currently, we are working on the simultaneous measurement of AFM profiles and optical thickness measurements in situ. This will provide a direct calibration of our system. However, the data presented here strongly suggest that the optical data are meaningful and provide accurate information about the spatial distribution of the rate of galvanic corrosion.

Corrosion Studies by Zero Resistance Ammetry. The IE for varying CTAB concentration calculated simply from the mean dissolution time was compared to ZRA measurements using a bulk copper electrode. We did so because the presence of a reaction product surface layer (see AFM results) indicates that the corrosion inhibition data measured optically needs to be verified with classical electrochemical techniques. Our galvanic model system provides the opportunity to partly separate anodic and cathodic contributions to the corrosion inhibition since the majority of the cathodic reaction (oxygen reduction) is taking place on the gold cathode. To mimic the conditions in our original setup as closely as possible, we chose ZRA as a quantitative method to measure the reaction rates in a copper−gold galvanic pair as a function of inhibitor concentration. However, a major difference in our original setup is the electrode geometry: Instead of plated copper islands on gold in a coplanar geometry, a high purity copper rod embedded in epoxy is employed as a working electrode. As a cathode, again an evaporated gold thin film is used. Thus, inhibition data measured with ZRA can only qualitatively be compared to our optical results.

For the ZRA measurements, copper anode and gold cathode are located in separate baths with a KCl salt bridge connecting the two half cells. The current densities as a function of CTAB concentration are shown in Figure 3c. Three different kinds of experiments were performed, where CTAB was applied either only to the cathodic half cell, only to the anodic half cell, or to both half cells simultaneously.

When CTAB is added solely to the copper electrode half cell, corrosion inhibition is observed only at a concentration below 0.2 mM. At larger concentrations, the current density increases as the concentration of CTAB in solution increases (Figure 3c). Thus, applied to the anode alone, CTAB promotes the corrosion of copper coupled to a gold cathode. The increase of corrosion rate occurs already at CTAB concentrations below the CMC.

If only the gold half cell is exposed to the surfactant, the current density decreases as CTAB is added to the electrolyte. For any CTAB concentration between 0.4 mM (which is supposedly slightly below or at the bulk CMC) and 15 mM (which is well above the bulk CMC), we observe approximately the same low current density. This shows that, because of the presence of the surfactant, the cathode is poisoned and even at high surfactant concentrations no reaction enhancement occurs. Wanless and Ducker[25] showed for another surfactant that a full surface coverage can be achieved even at bulk concentrations well below the CMC. This might also apply to our system, and we assume that the observed constancy of the current density is caused by the formation of complete surfactant layer at a bulk CTAB concentration around 0.4 mM.

When CTAB is added to both the copper and the gold electrode half cell, the current density decreases initially and then increases as the CTAB concentration is increased beyond 0.2 mM. Thus, there is a minimum in dissolution rate, similar to what we observed in our optical experiments. The position of the minimum probably lies between 0.1 and 0.4 mM and is shifted toward lower concentrations compared to the minimum observed in the optical experiments (Figure 2c).

We conclude that this minimum is caused by the superposition of the effects the surfactant has on anodic and cathodic sites. While applied to the cathode only, inhibitory effects are observed which saturate as a sufficiently high concentration is reached. On the other hand, CTAB has a detrimental effect on the anodic sites. Since with increasing CTAB concentration the inhibition on the cathode remains constant, but corrosion-promoting effects on the copper anode increase further, a minimum of dissolution rate of copper is observed.

We believe that the overall inhibition of corrosion in our galvanic couple is at its maximum when a full coverage of the cathode is achieved. Up to this point, the inhibitory effects on cathode and anode dominate over the corrosion enhancement caused by halide ions on the anode. If we increase the CTAB concentration beyond a value of about 0.4 mM, the surface coverage on the cathode cannot increase further. Instead, the increasing concentration of halide ions on the copper anode catalyzes the copper dissolution reaction further and leads to a higher reaction rate. We assume that the mechanism leading to a minimum in dissolution rate as a function of CTAB concentration in the microreactor is qualitatively the same as that leading to a minimum dissolution rate in the bulk ZRA experiments.

It is important to keep in mind that there are clear differences in the geometry between bulk electrode experiments and the microreactor experiments: Electrodes in the microreactor are coplanar and are located right next to each other, whereas in the bulk systems electrodes are completely separate and are located on opposite ends of the electrochemical cell. This leads to differences in current and potential distribution on electrodes for the two experimental setups, and transport paths of ions from one electrode to the other differ. However, since the minimum in dissolution rate is observed for both sets of experiments, we propose that these differences do not change the qualitative result.

Corrosion IEs in the microsystem and ZRA experiments differs substantially. While we obtain a maximum IE of 99.5% for the microsystem, from the ZRA results we can calculate a maximum IE of about 75%. This discrepancy can (at least partly) be explained by the different reaction rate we observe in the two systems. In the microsystem, the ionic current has to flow only a distance of a few tens of micrometers through the electrolyte because cathode and anode are located in immediate proximity to each other. The cell resistance is low. On the contrary, in the ZRA experiments with separated half cells, the ionic current has to flow through macroscopic amounts of electrolyte and the salt bridge. Thus, the cell resistance is comparably high, and already in the absence of the surfactant the current density is low. Accordingly, corrosion inhibition appears to be less efficient.

Conclusions

We developed an optical microscopy-based method for the analysis of corrosion kinetics of metal thin films. As long as color variations are not affected by the formation of adlayers (reaction products) on the anode, our method can be used as a powerful quantitative tool for measuring corrosion rates with high spatial and temporal resolution in microscopic model

systems. The technique is, of course, not limited to copper−gold galvanic pairs, but can as well be applied to other, technically more relevant material pairs such as copper and aluminum, metal−semiconductor pairs, or metal thin films on inert surfaces.

While our optical method cannot provide quantitative data about the corrosion rate in a situation where reaction products form on the dissolving anode, it provides qualitative information about the corrosion inhibition efficiency of certain corrosion inhibitors. Solely on the basis of our optical results, in an electrochemical cell configuration which is hardly accessible for classical electrochemical methods, we found both a minimum in dissolution rate as a function of inhibitor concentration and indication for the formation of reaction product layers in our system. We observed the same minimum in dissolution rate for ZRA measurements done on bulk electrodes, and this confirms (qualitatively) results from the optical method. With ZRA measurements we explain why there is a minimum in dissolution rate as a function of CTAB concentration and infer that the same mechanism is responsible for the minimum observed in microreactor experiments. More specifically, our experiments with separated half cells show that CTAB promotes the corrosion of copper in a copper−gold galvanic pair which is most likely due to the catalytic action of bromide counterions on the copper surface.[52] These measurements also show that CTAB inhibits the reaction taking place on the gold electrode. These two competing processes lead to the minimum in dissolution rate as a function of CTAB concentration.

Acknowledgment. This work was supported by ARO/MURI under Grant No. W911NF-04-1-0170, and NASA University Research, Engineering, and Technology Institute on BioInspired Materials (BIMat) under Award No. NCC-1-02037. C.P. acknowledges support by the Alexander von Humboldt Foundation.

Supporting Information Available: Calibration details and ex situ FTIR measurements. This material is available free of charge via the Internet at http://pubs.acs.org.

LA8024759